NASA TECHNICAL NOTE

NASA TN D-5185

SIGMA PHASE FORMATION AND ITS EFFECT ON STRESS-RUPTURE PROPERTIES OF IN-100

by Robert L. Dreshfield and Richard L. Ashbrook

Lewis Research Center
Cleveland, Ohio

NATIONAL AERONAUTICS AND SPACE ADMINISTRATION • WASHINGTON, D. C. • APRIL 1969

NASA TN D-5185

SIGMA PHASE FORMATION AND ITS EFFECT ON STRESS-RUPTURE PROPERTIES OF IN-100

By Robert L. Dreshfield and Richard L. Ashbrook

Lewis Research Center
Cleveland, Ohio

NATIONAL AERONAUTICS AND SPACE ADMINISTRATION

For sale by the Clearinghouse for Federal Scientific and Technical Information
Springfield, Virginia 22151 – CFSTI price $3.00

ABSTRACT

Three IN-100 compositions, sigma-free to very sigma-prone, were made by adding aluminum and titanium to one master heat. At 1550° F (843° C), the sigma-free alloy had no sigma after 5000 hours; the very-sigma-prone alloy formed sigma in less than 24 hours. Sigma-prone alloys had rupture lives as low as 10 percent of that expected for sigma-free alloys in sigma-forming, temperature-time realms. Sigma phase had no discernible effect on rupture ductility. The use of time-temperature parameters in sigma-forming alloys was analyzed.

SIGMA PHASE FORMATION AND ITS EFFECT ON STRESS-RUPTURE PROPERTIES OF IN-100

by Robert L. Dreshfield and Richard L. Ashbrook

Lewis Research Center

SUMMARY

An investigation was conducted to determine the effect of sigma phase formation in the nickel-base alloy IN-100. One master heat of the alloy was modified, within the range of commercial specifications, by adding only aluminum and titanium to remelt heats to produce alloys with approximately 5 percent Al, 4.2 percent Ti; 5.5 percent Al, 4.3 percent Ti; and 5.5 percent Al, 4.6 percent Ti. Metallographically these alloys were sigma-free, moderately sigma-prone, and very sigma-prone, after exposure to temperatures between 1300° F (704° C) and 1800° F (982° C) for times to 5000 hours. The very-sigma-prone alloy formed sigma in less than 24 hours at 1550° F (843° C), while the sigma-free alloy formed none after 2500 hours at all the temperatures studied or after 5000 hours at 1550° F (843° C). The time to initiate sigma phase precipitation decreased, and the temperature range in which sigma phase was observed increased, as the aluminum and titanium concentrations were increased.

The sigma-prone alloys had shorter rupture lives than the sigma-free alloys in the sigma-forming, temperature-time realm. For example, at 30 000 psi (206 MN/m^2) and 1550° F (843° C) the very-sigma-prone alloy had approximately 10 percent of the life expected for the sigma-free alloy. No effect of sigma phase on rupture ductility was established.

The average electron vacancy number $\overline{N}_v$ of the residual matrix computed by two concepts of element partitioning, compared to reported critical average electron vacancy numbers, correctly predicted sigma phase occurrence.

For sigma-free IN-100, coarse-grained materials tended to have longer stress-rupture lives than fine-grained materials. The opposite was true for the sigma-prone alloys.

Analysis of methods for predicting stress-rupture life of IN-100 shows that the predictions can be in gross error in the sigma-forming realm. Such an error can occur if attempts are made to predict the life of one material by using data from another material of a different stability level.

INTRODUCTION

Recent developments in gas turbines require that materials be exposed to time-temperature realms not previously experienced in the industry. Consequently, an area of particular concern to metallurgists selecting materials for these engines is the microstructural stability of available materials and the changes in mechanical properties which may result from prolonged exposure to the operating environment. For example, it has long been recognized that chromium carbide tends to precipitate at grain boundaries of superalloys and cause embrittlement (ref. 1). It has also been reported that sigma phase can form in a Widmanstätten pattern in some nickel-base superalloys and may also embrittle these alloys (ref. 2).

The nickel-base alloy IN-100 possesses good high-temperature properties for use in advanced gas turbines; however, it has been reported that the alloy forms sigma phase when exposed to temperatures near 1600° F (871° C) (ref. 3). Recently, it has been reported that a loss of stress-rupture life accompanies the formation of sigma phase in this alloy (ref. 4). The tendency to form sigma phase can be controlled in IN-100 by maintaining compositions in ranges computed by a method called PHACOMP (ref. 5), which relates the average electron vacancy concentration $\overline{N}_v$ of the residual matrix of the alloy to the melt chemistry. If the $\overline{N}_v$ is below a critical value, the alloy is expected to be sigma-free after prolonged exposure at elevated temperature.

This investigation was initiated to determine the extent of stress-rupture degradation associated with sigma phase formation in IN-100 and the effect of composition and exposure conditions on sigma phase formation.

Coarse- and fine-grained investment cast test bars were made from remelts of a single master heat. Aluminum and titanium additions were made to the remelts to provide three materials with varying tendencies toward sigma formation. The aluminum and titanium additions were chosen to provide three $\overline{N}_v$ levels such that one alloy would be sigma-free, one moderately sigma-prone, and one strongly sigma-prone. The compositions melted lie within some commercial chemical specifications for IN-100, but were slightly lower in aluminum plus titanium content than the minimum specified by AMS 5397 (ref. 6). Specimens were aged between 1300° and 1800° F (704° and 982° C) for times to 5000 hours to determine the time to initiate sigma formation. Stress-rupture tests were conducted at stresses between 100 000 and 20 000 psi (689 and 138 MN/m^2) and at temperatures from 1300° to 1800° F (704° and 982° C) to determine the effect of sigma formation on the stress-rupture life.

PROCEDURE

Materials

Oversize investment cast test bars, made from remelt heats of a single master heat of IN-100, were purchased from a commercial foundry. At the time of casting, the compositions of the remelt heats were modified by additions of aluminum (Al) plus titanium (Ti). These additions resulted in materials with three different propensities toward sigma formation.

The specific additions were determined by using a phase computation method similar to that of Boesch and Slaney (see appendix). The target average electron vacancy concentrations $\overline{N}_v$ were 2.32 maximum, 2.42 to 2.47, and 2.50 minimum. The greater the aluminum plus titanium addition, the higher the $\overline{N}_v$. It was anticipated that the low-$\overline{N}_v$ alloy would be sigma-free and the other two would show an increasing propensity toward sigma formation with increasing $\overline{N}_v$. Compositions of randomly selected remelt heats of the alloys and two calculated $\overline{N}_v$ are shown in table I. The calculation of $\overline{N}_v$ by the method of Woodyatt, Sims, and Beattie is also described in the appendix. The low-$\overline{N}_v$ and medium-$\overline{N}_v$ alloys had slightly lower aluminum plus titanium content than specified by AMS 5397 (ref. 6) but were within the range allowed by some commercial specifications. All alloys were cast by normal investment casting procedures; however, some molds were inoculated to provide fine-grained material. Typical examples of the

TABLE I. - TYPICAL CHEMICAL ANALYSES OF IN-100

Alloy type	Element, wt. % (balance Ni)											Average electron vacancy concentration, $\overline{N}_v$	
	Co	Cr	Al	Ti	Mo	V	Si	Fe	Zr	C	B	(a)	(b)
Low $\overline{N}_v$	13.58	10.26	4.95	4.10	3.45	0.96	0.08	0.07	0.02	0.160	0.014	2.14	2.27
	13.48	10.13	5.03	4.22	3.65	1.01	.08	.14	.04	.176	.015	2.19	2.31
Medium $\overline{N}_v$	13.29	10.15	5.47	4.28	3.51	0.96	0.10	0.07	0.03	0.160	0.014	2.29	2.47
	13.35	10.13	5.51	4.30	3.60	.96	.10	.07	.03	.164	.013	2.31	2.51
High $\overline{N}_v$	13.22	10.11	5.55	4.59	3.50	0.96	0.11	0.06	0.03	0.157	0.014	2.37	2.59
	13.29	10.13	5.65	4.78	3.53	.98	.09	.08	.03	.158	.012	2.45	2.71
AMS 5397:													
Minimum	13.00	8.00	[c]5.00	[c]4.50	2.00	0.70	----	----	0.03	0.15	0.01	----	----
Maximum	17.00	11.00	6.00	5.00	4.00	1.20	0.15	1.00	.09	.20	.02	----	----

[a]Method of Boesch and Slaney (see appendix). Critical $\overline{N}_v$ = 2.32.
[b]Method of Woodyatt, Sims, and Beattie (see appendix). Critical $\overline{N}_v$ = 2.46.
[c]Al + Ti > 10.0.

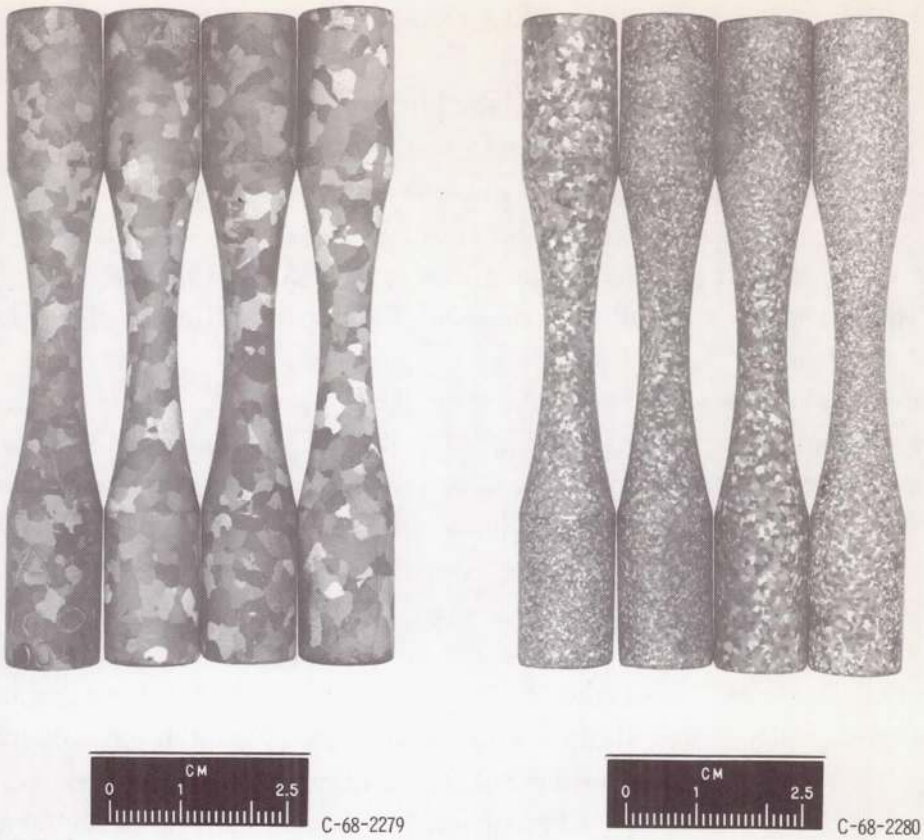

(a) Coarse grain size.

(b) Fine grain size.

Figure 1. - Surface grain size of cast test bars of IN-100.

surface grain size on macroetched bars from untreated and from inoculated molds are shown in figure 1.

Mechanical Testing

All data in this report were obtained from specimens in the as-cast condition. Tensile tests and constant load stress-rupture tests were conducted on the alloy in accordance with appropriate ASTM standards. The test bar shown in figure 2 was used for both tensile and stress-rupture testing. The oversize cast specimens were ground to a nominal 1/4-inch- (0.6-cm-) diameter at the test section.

A gage length was defined by marks 1.75 inches (4.51 cm) apart placed on the shanks of the specimen. The effective gage length was taken as the distance between the base of the fillets. The elongation was then calculated from the following equation:

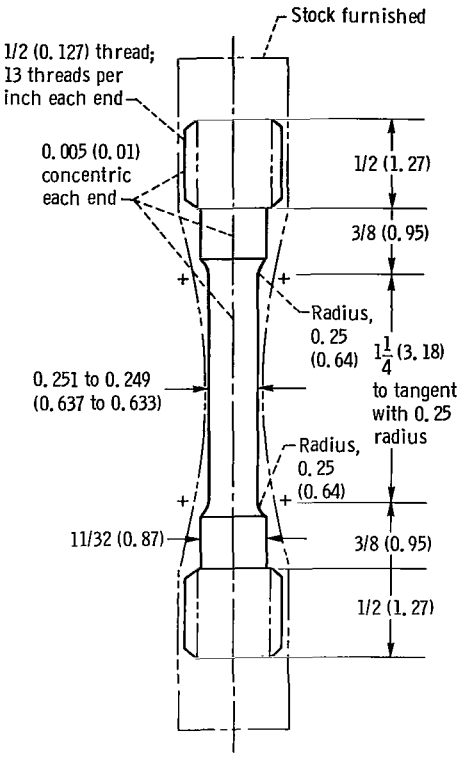

Figure 2. - Test specimen. Dimensions are in inches (cm).

$$\%E = \frac{\text{Final GL - Original GL}}{\text{Effective GL}} \times 100 \qquad (1)$$

where GL is gage length.

Stress-rupture specimens were heated to the test temperature in 3 to 5 hours and soaked an additional 1 to 2 hours prior to loading. Care was taken not to exceed the test temperature during heating.

Aging

As-cast tensile specimens were cut in half transversely through the gage section to make isothermal transformation specimens. These specimens were heated with no applied stress at temperatures from 1300° to 1800° F (704° to 982° C) for times ranging from 24 to 5000 hours. An argon atmosphere was used to prevent excessive oxidation.

Metallography

Specimens used for the isothermal transformation study and stress-rupture specimens which had broken under load were examined metallographically for the presence of sigma. An etchant having the following composition in milliliters: 33 water (H_2O), 33 nitric acid (HNO_3), 33 acetic acid (H_3CH_3COOH), 1 hydrofluoric acid (HF) (mixed acid etch) revealed sigma under polarized light as an optically active constituent on a dark field. A second etch of 60 milliliters each of the solutions: 10 grams of potassium ferrocyanide ($K_4Fe(CN)_6$) in 90 milliliters H_2O and 10 grams of potassium hydroxide (KOH) in 90 milliliters H_2O (modified Murakami's etch) was used to reveal sigma and carbides without attacking other phases.

Extracted residues of selected samples were analyzed by X-ray diffraction to confirm the presence of sigma. The residues were extracted using 10 percent bromine-methanol or 10 percent hydrochloric acid - methanol. The HCl-methanol extraction was conducted electrolytically.

RESULTS AND DISCUSSION

Unstressed Isothermal Formation of Sigma

To determine the kinetics of the start of sigma precipitation, samples were heated to temperatures from 1300° to 1800° F (704° to 982° C) for times varying from 24 to 5000 hours. Metallographic examination of the isothermal transformation specimens with the mixed acid etch revealed all the common structural features in the alloy. The monocarbides (MC) were tinted a slate color, and the sigma phase exhibited optical activity under polarized light. Figures 3(a) to (d) are time temperature transformation (TTT) curves of the medium- and high-$\overline{N}_v$ alloys in both grain sizes. They show the onset of sigma formation as determined by metallographic examination with the mixed acid etch. Analysis by X-ray diffraction of residues extracted from selected samples confirmed the presence of sigma in samples showing optically active Widmanstätten structures. No sigma was detected in samples not showing a Widmanstätten structure. It is assumed at this writing that sigma is the only phase forming the Widmanstätten pattern in IN-100. No TTT curve is shown for the low-$\overline{N}_v$ material, since sigma was not observed in any of the samples examined.

The TTT curves are plotted on a reciprocal absolute temperature scale to allow the calculation of activation energies for the rate-controlling process for nucleation (ref. 7). However, the activation energies found from this analysis do not correspond well with those of any reported diffusional process in nickel alloys.

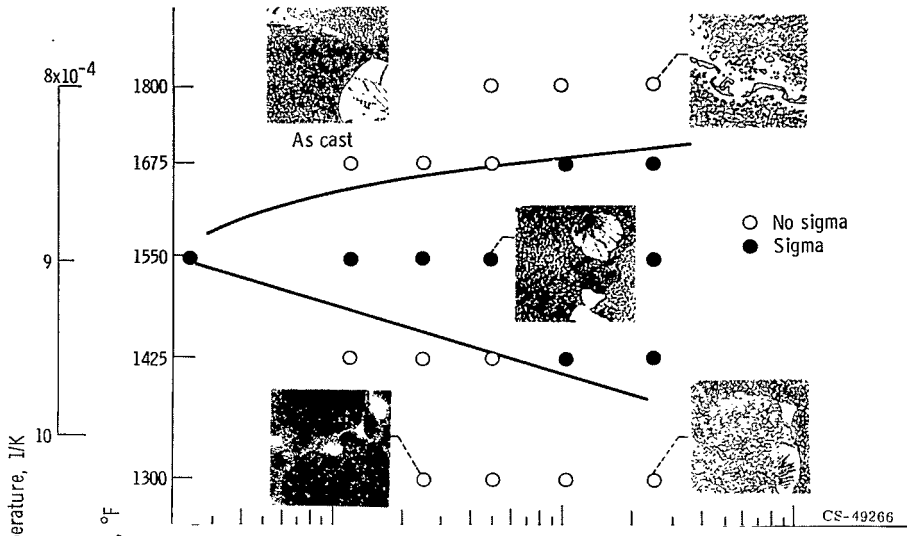

(a) Medium average electron vacancy concentration $\bar{N}_v$, fine grain size.

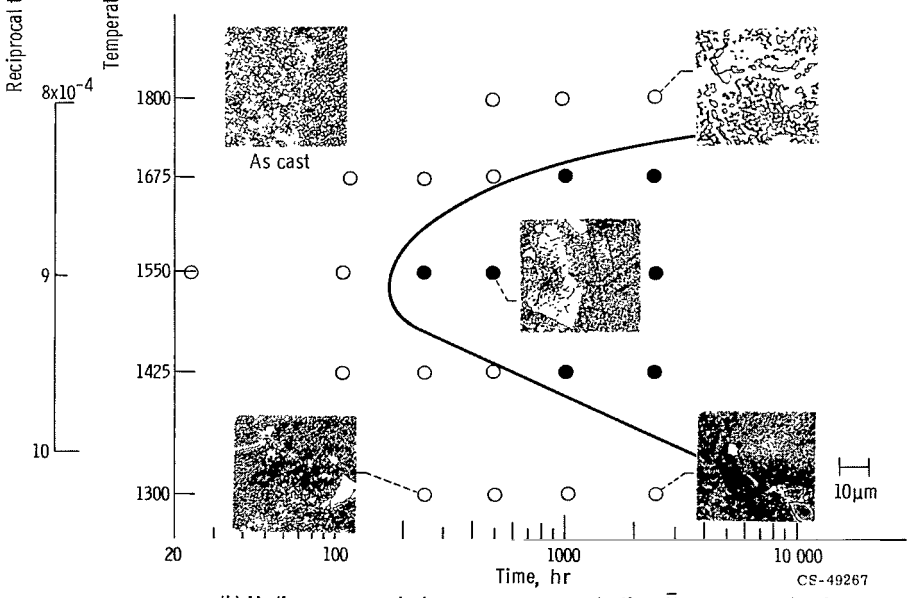

(b) Medium average electron vacancy concentration $\bar{N}_v$, coarse grain size.

Figure 3. - Unstressed isothermal transformation of IN-100.

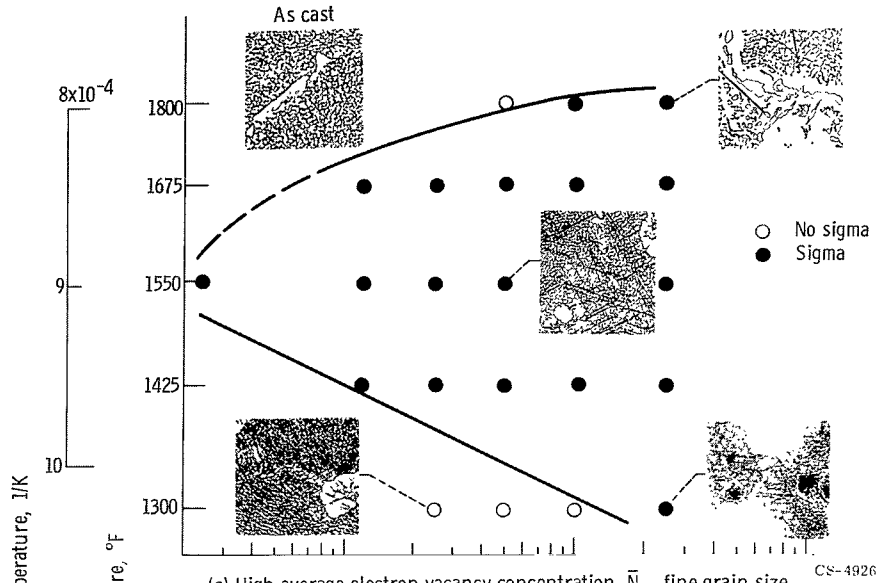

(c) High average electron vacancy concentration $\bar{N}_V$, fine grain size.

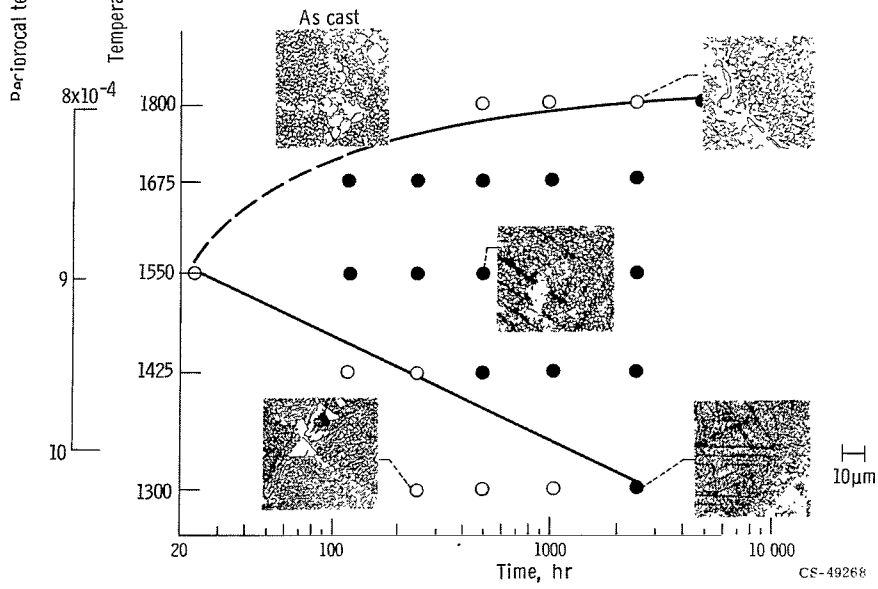

(d) High average electron vacancy concentration $\bar{N}_V$, coarse grain size.

Figure 3. - Concluded.

It is apparent that the time to start sigma precipitation was greatly reduced as the $\overline{N}_v$ increased. It is further apparent that the temperature range over which sigma will form was increased as the $\overline{N}_v$ increased. An effect of grain size on the formation of sigma phase for a constant $\overline{N}_v$ was also observed. For the high-$\overline{N}_v$ alloy, the start of sigma formation was retarded in the coarse-grained material at 1425° and 1800° F (774° and 982° C). The same trends were also observed in the medium-$\overline{N}_v$ material at 1550° F (843° C); at 1550° F (843° C), the nose of the curve occurred in less than 24 hours for the fine-grained alloy and in more than 100 hours for the coarse-grained alloy.

Mechanical Properties

Tensile tests. - The results of room-temperature tensile tests conducted on as-cast material are listed in table II. All material met AMS 5397 minimum requirements for

TABLE II. - ROOM-TEMPERATURE TENSILE PROPERTIES OF AS-CAST IN-100

Alloy type[a]	Ultimate tensile strength		0.2 Percent yield strength		Elongation, percent	Reduction in area, percent
	psi	MN/m^2	psi	MN/m^2		
LF	138 100	952	101 100	697	9	10
LF	145 600	1004	102 600	707	15	12
MF	151 500	1045	107 300	740	12	11
MF	154 900	1068	117 700	812	7	6
HF	131 400	906	96 700	667	6	7
HF	153 700	1060	(b)	(b)	12	11
LC	139 900	965	97 800	674	9	9
LC	144 400	996	107 300	740	9	9
MC	131 600	907	104 700	722	7	9
MC	125 700	867	95 100	656	7	9
HC	130 000	896	106 800	736	3	6
HC	126 500	872	105 500	727	4	6
AMS 5397 (minimum)	115 000	793	95 000	655	5	--

[a]LF, low $\overline{N}_v$, fine grain size; MF, medium $\overline{N}_v$, fine grain size; HF, high $\overline{N}_v$, fine grain size; LC, low $\overline{N}_v$, coarse grain size; MC, medium $\overline{N}_v$, coarse grain size; HC, high $\overline{N}_v$, coarse grain size.

[b]Not determined.

TABLE III. - STRESS-RUPTURE DATA FOR IN-100

Temperature		Stress		Life, hr	Reduction in area, percent	Elongation, percent
°F	°C	psi	MN/m^2			
Low $\overline{N}_v$, fine grain size						
1300	704	100×10^3	689	1031.3	3	5
↓	↓	100	689	509.4	11	4
↓	↓	100	689	124.9	7	8
↓	↓	95	654	696.3	9	8
↓	↓	↓	↓	1208.1	6	3
1360	738	↓	↓	203.3	3	4
1360	738	↓	↓	277.3	5	5
1425	774	↓	↓	34.5	3	4
↓	↓	↓	↓	41.6	3	4
↓	↓	70	482	1315.8	5	5
↓	↓	↓	↓	1140.2	9	7
1500	816	↓	↓	191.4	12	7
1500	816	↓	↓	199.5	3	4
1550	843	↓	↓	49.9	8	9
↓	↓	↓	↓	41.8	11	8
↓	↓	50	344	439.3	18	7
↓	↓	↓	↓	528.4	10	12
1625	885	↓	↓	110.1	10	6
1625	885	↓	↓	123.1	8	9
1675	913	↓	↓	33.8	9	9
1700	927	↓	↓	11.0	10	9
1700	927	↓	↓	9.1	8	8
1700	927	↓	↓	7.5	12	12
1550	843	40	276	2372.7	9	(a)
1550	843	↓	↓	861.3	9	11
1575	857	↓	↓	1546.5	--	--
1625	885	↓	↓	423.2	8	11
1625	885	↓	↓	456.3	9	11
1675	913	↓	↓	127.9	9	8
1675	913	↓	↓	115.7	6	9
1675	913	↓	↓	67.2	9	11
1600	871	30	206	2866.2	13	12
1600	871	↓	↓	3324.5	(a)	(a)
1675	913	↓	↓	579.6	9	14
1675	913	↓	↓	541.6	10	10
1725	941	↓	↓	147.0	13	10
1725	941	↓	↓	131.6	15	12
1800	982	↓	↓	18.7	14	15
1800	982	↓	↓	22.3	10	10
1675	913	25	172	1336.7	9	9
1675	913	25	172	1263.3	13	11
1800	982	20	138	242.0	13	11
1800	982	20	138	210.6	18	13

Temperature		Stress		Life, hr	Reduction in area, percent	Elongation, percent
°F	°C	psi	MN/m^2			
Low $\overline{N}_v$, coarse grain size						
1300	704	100×10^3	689	385.3	5	5
↓	↓	↓	689	270.1	3	3
↓	↓	↓	689	649.2	5	5
↓	↓	95	654	1402.6	4	5
↓	↓	95	654	1227.2	5	4
1550	843	70	482	34.8	6	4
↓	↓	70	482	36.9	2	6
↓	↓	60	413	250.7	7	8
↓	↓	60	413	213.0	5	8
↓	↓	40	276	1720.8	15	12
↓	↓	↓	↓	3040.1	6	3
1675	913	↓	↓	112.3	7	32
1675	913	↓	↓	154.9	8	6
1600	871	30	206	3719.2	2	5
1675	913	↓	↓	595.1	4	9
1675	913	↓	↓	546.1	9	8
1800	982	↓	↓	29.3	10	8
1800	982	↓	↓	31.5	7	8
1675	913	25	172	1455.0	6	7
1675	913	25	172	1220.3	8	9
Medium $\overline{N}_v$, fine grain size						
1300	704	100×10^3	689	331.2	4	2
↓	↓	100	689	502.1	4	3
↓	↓	95	654	1145.6	3	4
↓	↓	↓	↓	1599.1	6	6
1360	738	↓	↓	223.0	3	3
1360	738	↓	↓	225.5	6	6
1360	738	↓	↓	131.2	2	2
1425	774	↓	↓	30.2	3	4
1425	774	↓	↓	41.1	4	3
1425	774	70	482	1178.8	6	4
1500	816	↓	↓	234.1	6	6
1500	816	↓	↓	193.3	4	5
1550	843	↓	↓	20.6	2	3
↓	↓	↓	↓	64.9	6	6
↓	↓	↓	↓	82.9	10	10
↓	↓	50	344	421.6	12	9
1500	816	↓	↓	1080.3	6	7
1500	816	↓	↓	1088.1	10	7
1550	843	↓	↓	603.8	7	7
1550	843	↓	↓	[b]386.8	2	4
1625	885	↓	↓	104.8	5	6
1625	885	↓	↓	117.1	6	7
1700	927	↓	↓	20.7	8	9
1550	843	40	276	714.2	13	11
1550	843	↓	↓	815.8	10	6
1625	885	↓	↓	396.6	9	9
1625	885	↓	↓	378.4	10	9
1675	913	↓	↓	118.4	9	9
1675	913	↓	↓	134.3	10	8
1600	871	30	206	1649.9	10	7
1600	871	↓	↓	1620.7	5	8
1675	913	↓	↓	497.2	9	8
1675	913	↓	↓	511.8	9	8
1725	941	↓	↓	184.9	6	10
1725	941	↓	↓	191.7	7	9
1800	982	↓	↓	35.0	5	7
1800	982	↓	↓	29.9	6	7
1800	982	↓	↓	32.2	10	9
1675	913	25	172	1106.9	6	7
1675	913	25	172	1334.5	7	8
1800	982	20	138	268.8	8	6
1800	982	20	138	293.0	7	8

[a]Bad fit of fracture; value not determined.

[b]Timer failed to turn off, time 386.8 to 450.8 hr.

TABLE III. - Concluded. STRESS-RUPTURE DATA FOR IN-100

Temperature		Stress		Life, hr	Reduction in area, percent	Elongation, percent
°F	°C	psi	MN/m^2			
Medium $\bar{N}_v$, coarse grain size						
1300	704	100×10^3	689	341.8	6	5
↓	↓	↓	689	227.1	4	5
			689	109.1	2	2
		95	654	460.5	6	3
↓	↓	95	654	462.7	5	4
1550	843	70	482	27.0	5	6
↓	↓	70	482	23.4	2	3
		60	413	112.1	5	5
		60	413	123.7	5	6
		46	322	591.6	3	4
↓	↓	46.8	276	473.5	1	1
1675	913	40	276	120.1	5	7
1675	913	40	276	106.3	6	8
1600	871	30	206	1468.2	2	4
1600	871	↓	↓	1195.5	2	3
1600	871			1915.6	5	5
1675	913			427.6	4	5
1675	913			615.9	6	9
1800	982			30.0	6	8
1800	982	↓	↓	15.6	5	8
1675	913	20	138	3201.7	9	9
1675	913	25	172	1102.0	2	8
High $\bar{N}_v$, fine grain size						
1300	704	100×10^3	689	275.9	2	3
↓	↓	100	689	176.1	2	2
		95	654	855.5	5	5
↓	↓	↓	↓	381.1	2	3
1360	738			71.9	3	3
1360	738			138.5	2	4
1425	774			15.4	3	3
1425	774	↓	↓	22.7	6	5
1390	754	70	482	936.5	6	6
1390	754	↓	↓	714.4	2	3
1425	774			385.9	5	3
1425	774			435.8	3	3
1500	816			54.4	2	2
1500	816			95.7	4	4
1550	843			24.6	1	2
1550	843	↓	↓	39.1	6	5
1550	843	50	344	194.5	12	8
1625	885	50	344	42.9	3	5
1625	885	50	344	49.8	2	3
1475	802	40	276	1494.0	11	11
1475	802	↓	↓	1200.0	14	(a)
1550	843			320.8	3	5
1550	843	↓	↓	319.6	9	6

Temperature		Stress		Life, hr	Reduction in area, percent	Elongation, percent
°F	°C	psi	MN/m^2			
High $\bar{N}_v$, fine grain size (concluded)						
1625	885	40×10^3	276	130.9	5	5
1625	885	↓	↓	86.2	2	2
1675	913			27.8	4	3
1675	913	↓	↓	61.1	6	6
1500	816	30	206	2089.7	15	13
1500	816	↓	↓	2105.3	10	9
1525	829			1257.9	3	9
1525	829			1111.1	8	9
1550	843			814.7	11	9
1550	843			685.4	6	6
1575	857			499.7	12	12
1575	857			580.3	8	9
1600	871			414.4	9	9
1600	871			385.8	12	9
1675	913			173.9	7	7
1675	913			150.2	3	3
1725	941			85.8	4	5
1725	941			96.3	2	4
1800	982			23.1	3	4
1800	982	↓	↓	27.0	6	6
1675	913	25	172	335.3	7	6
1675	913	25	172	329.0	6	5
1800	982	20	138	280.0	6	7
1800	982	20	138	214.8	8	8
High $\bar{N}_v$, coarse grain size						
1300	704	100×10^3	689	96.7	11	7
↓	↓	100	689	6.0	1	1
		100	689	135.7	2	3
		95	654	435.9	3	4
↓	↓	95	654	348.5	7	4
1550	843	70	482	31.3	6	5
↓	↓	70	482	6.4	1	2
		60	413	73.3	3	4
		60	413	75.5	4	6
		40	276	326.6	6	4
↓	↓	↓	↓	309.1	2	5
1675	913			50.9	2	3
1675	913	↓	↓	37.2	1	2
1600	871	30	206	410.6	8	8
1600	871	↓	↓	489.8	10	8
1675	913			141.1	3	3
1675	913			155.1	3	4
1800	982			14.8	5	2
1800	982	↓	↓	25.6	3	4
1675	913	25	172	377.2	6	5
1675	913	25	172	480.8	7	5

[a]Bad fit of fracture; value not determined.

IN-100 except the coarse-grained, high-$\overline{N}_v$ material which had 3 to 4 percent elongation compared to a minimum specified value of 5 percent. In general, the coarse-grained material appeared to be somewhat less ductile than the fine-grained material of a given $\overline{N}_v$, and the ductility tended to decrease with increasing $\overline{N}_v$. (This decrease is probably due to an increase in gamma prime as the Al and Ti were increased.)

Stress-rupture tests. - The results of stress-rupture tests made at temperatures between 1300° and 1800° F (704° and 982° C) with stress varying from 100 000 to 20 000 psi (689 to 138 MN/m^2) for both coarse- and fine-grained materials are shown in table III. Because the results are similar for both grain sizes, figures 4 and 5 show isostress diagrams of the stress-rupture data for only the fine-grain-size material. It can be seen (fig. 4) that log time to rupture of the low-$\overline{N}_v$ material conforms well to a linear function of temperature. The medium- and high-$\overline{N}_v$ materials show considerable deviation from this behavior particularly at those temperatures and times where appreciable quantities of sigma phase formed (fig. 5). The deviation was generally toward that of reduced life when compared to the low-$\overline{N}_v$ alloy. This behavior is shown more

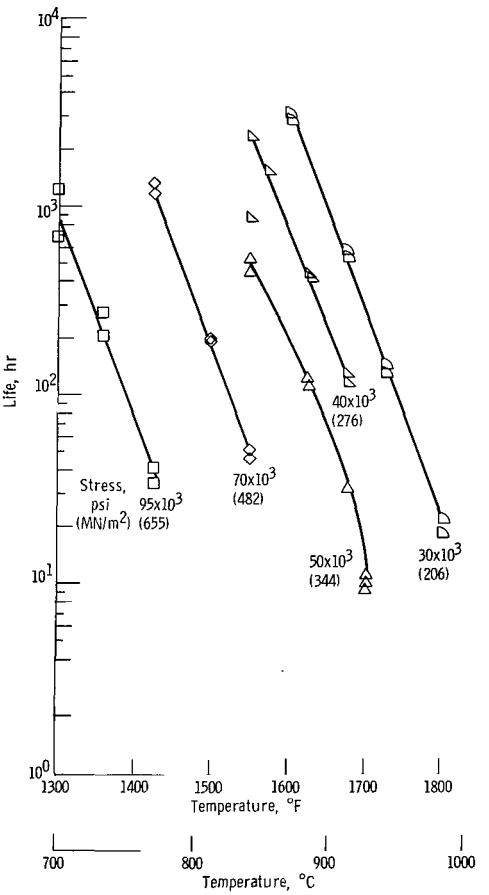

Figure 4. - Stress-rupture life of IN-100, low average electron vacancy concentration $\overline{N}_v$, fine grain size, as cast.

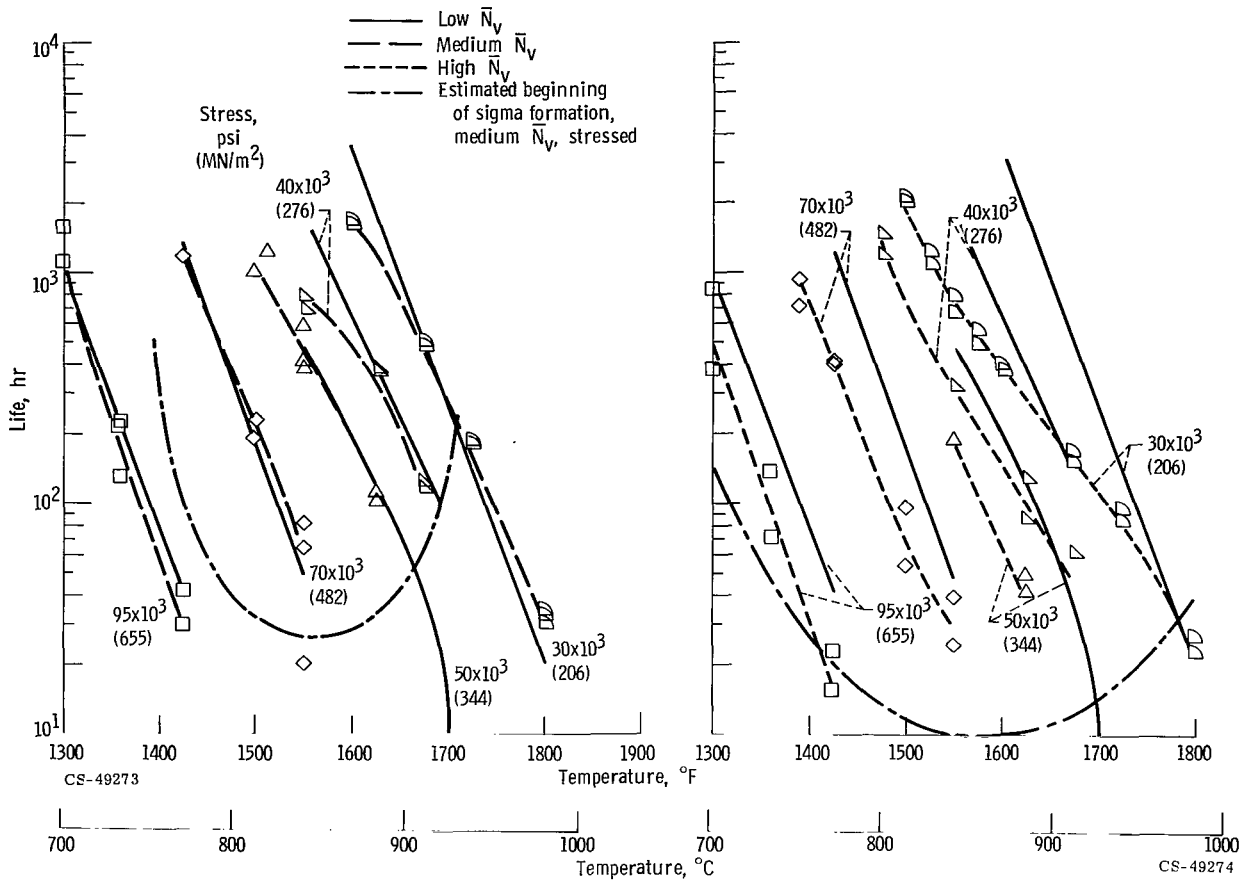

(a) Low and medium average electron vacancy concentrations $\bar{N}_v$.

(b) Low and high average electron vacancy concentrations $\bar{N}_v$.

Figure 5. - Comparison of stress-rupture life of IN-100, fine grain size, as cast.

clearly in figure 6 in which the geometric mean of rupture life for fine-grained material of medium- and high-$\bar{N}_v$ alloys was normalized against the life of the low-$\bar{N}_v$ alloy. The low- and medium-$\bar{N}_v$ alloys had similar rupture lives (life ratio of about 1) between 1360° and 1600° F (738° and 871° C) at stresses between 95 000 and 50 000 psi (655 and 344 MN/m^2). At temperatures of 1550° and 1600° F (843° and 871° C) with stresses of 40 000 and 30 000 psi (276 and 206 MN/m^2), respectively, the medium-$\bar{N}_v$ alloy had only 52 and 48 percent of the life of the low-$\bar{N}_v$ alloy. As the test temperature increased, the medium-$\bar{N}_v$-alloy life increased relative to that of the low-$\bar{N}_v$ alloy, so that above 1700° F (927° C) the low-$\bar{N}_v$ alloy failed in shorter times than the medium-$\bar{N}_v$ alloy. A similar comparison between the high-$\bar{N}_v$ and low-$\bar{N}_v$ alloys is even more dramatic. For example, at 1525° F (829° C) and 30 000 psi (206 MN/m^2) the high-$\bar{N}_v$ alloy has less than 10 percent of the life expected from the low-$\bar{N}_v$ alloy. To make this comparison, life values below 1600° F (871° C) were extrapolated for the low-$\bar{N}_v$-alloy,

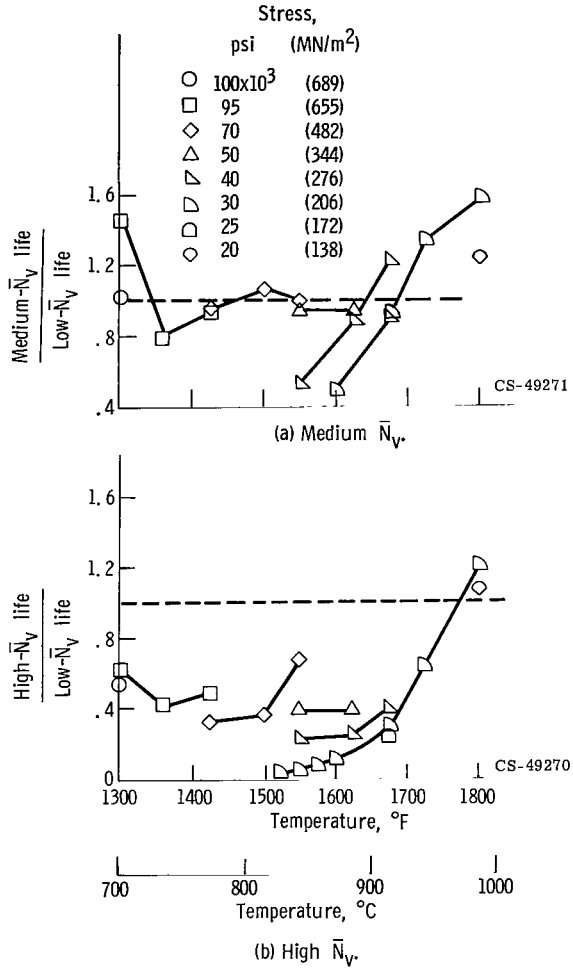

Figure 6. - Effect of temperature and stress on stress-rupture life ratio of IN-100, fine grain size.

30 000-psi (206-MN/m^2) isostress. Only at 1800° F (982° C) did the high-$\overline{N}_v$ alloy have a longer life than the low-$\overline{N}_v$ alloy. The low-$\overline{N}_v$ alloy was observed to be sigma-free at all temperatures and times studied, and the other alloys show the greater deviation in rupture life from the low-$\overline{N}_v$ alloy where sigma forms. Therefore, it is reasonable to assume that the loss in stress-rupture life observed is associated with the occurrence of the sigma phase.

It is not clear, however, from these data, whether the shorter rupture lives of the medium- and high-N_v alloys are the result of the presence of sigma or the formation of sigma during testing. Inspection of the 30 000-psi (206-MN/m^2) isostress curve for the high-$\overline{N}_v$ alloy (fig. 5(b)) reveals an inflection point (concave down to concave up) with decreasing temperature in the vicinity of 1600° F (871° C) at 350 hours. The curve then tends to become parallel to the low-$\overline{N}_v$ alloy line as the temperature decreases and time increases. The rate of sigma formation at the time of fracture in the high-$\overline{N}_v$ alloy should be decreasing with increasing time, below the temperature where the inflection occurs. This relation can be inferred from the sigma phase TTT curves, unstressed (fig. 3(c)) and stressed, as determined from tested stress-rupture bars, (fig. 5(b)). We might, therefore, speculate that the decrease in stress-rupture life observed for the 30 000-psi (206-MN/m^2) isostress line with decreasing temperature (fig. 5(b)) is associated with the formation of sigma, as opposed to its mere presence. This is further supported by the work done by Henry Collins of TRW under Air Force contract AFB3-615-5126 in which an increase in stress-rupture life was observed in an experimental alloy in which the sigma was formed prior to rupture testing.

A comparison of the effect of grain size on rupture life is shown in table IV. There does not appear to be any systematic effect of grain size as a function of either temperature or stress. The coarse-grained medium- and high-$\overline{N}_v$ alloys, however, generally

TABLE IV. - EFFECT OF GRAIN SIZE ON STRESS-RUPTURE LIFE OF IN-100

Temperature		Stress		Ratio of coarse-grain life to fine-grain life		
°F	°C	psi	MN/m^2	Low $\overline{N}_v$	Medium $\overline{N}_v$	High $\overline{N}_v$
1300	704	100×10^3	689	1.01	0.50	0.54
1300	704	95	654	1.43	.34	.68
1550	843	70	482	.78	.54	.46
1550	843	40	276	1.60	.62	.99
1600	871	30	206	1.12	.93	1.12
1675	913	40	276	1.28	.90	1.06
1675	913	30	206	1.02	1.02	.89
1675	913	25	172	1.02	.91	1.28
1800	982	30	206	1.49	.67	.78

show poorer stress rupture lives than the fine-grained material, whereas the opposite was shown for the low-$\overline{N}_v$ alloy.

Inspection of table III reveals that increasing the aluminum and titanium levels in the alloy decreases the stress-rupture ductility of the alloy. The data fail to show any change in ductility that can be uniquely associated with sigma phase, because the ductility of the alloys containing high levels of aluminum and titanium decreased even in realms where no sigma formed.

PREDICTION OF STRESS-RUPTURE LIFE

As was shown in the section Stress-rupture tests, the lives of unstable IN-100 fell far below the lives of stable IN-100 in the time-temperature realms where sigma formation occurred. There a comparison was made between the stable and unstable materials on the basis of isostress plots. Even though the high- and low-$\overline{N}_v$ IN-100 materials were nominally the same alloy, they behaved like two entirely different alloys in the sigma-forming realm.

Obviously, whatever criterion was used to predict life of sigma-prone IN-100 on the basis of sigma-free IN-100 data, the actual life would be very seriously overestimated, and the converse. For example, a commonly used method for predicting rupture life is extrapolation of isothermal plots of rupture data. Figure 7 shows curves for sigma-free (low $\overline{N}_v$) and sigma-prone (high $\overline{N}_v$) IN-100 at 1550° and 1675° F (843° and 913° C). Even in the relatively short times (up to 3000 hr) for which data were obtained, a life prediction based on the sigma-free-alloy data could dangerously overestimate the life of

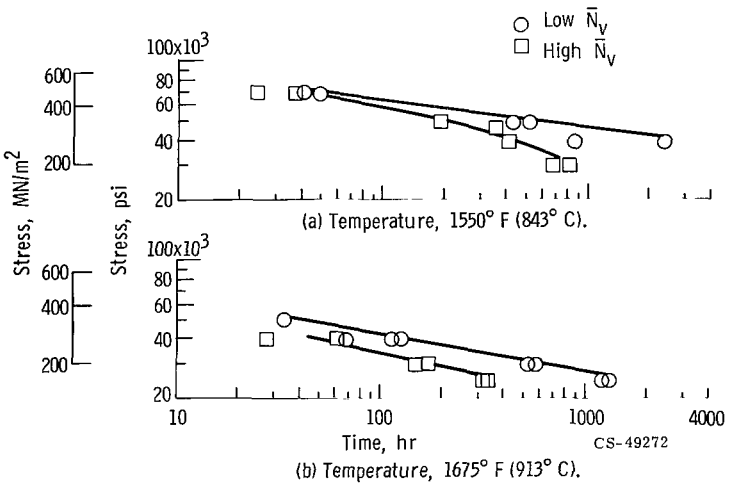

Figure 7. - Isothermal comparison of stress-rupture life of fine-grained low and high average electron vacancy $\overline{N}_v$ concentration.

the sigma-prone alloy. The divergence apparent in the 1550° F (843° C) curves would cause the error in prediction to become greater the longer the predicted life.

Parametric methods of predicting stress-rupture life of alloys are also widely used. Metallurgical instabilities can cause the same errors to occur in estimating the stress-rupture life of alloys like IN-100 by parametric methods as by more direct extrapolation methods. To emphasize this, a detailed examination of the Larson-Miller parametric method follows.

Optimum constants C for the Larson-Miller parameter

$$P = (T + 460)(\log t + C)$$

were calculated for each of the six types of alloy (i.e., low-$\overline{N}_V$, fine grain size; medium-$\overline{N}_V$, coarse grain size; etc.). These constants for the fine-grained alloys are listed in table V. The optimum constants calculated using the method of Mendelson, Roberts, and Manson (ref. 8) varied from 12.4 for the high-$\overline{N}_V$, fine-grained alloy to 20.0 for the low-$\overline{N}_V$, coarse-grained alloy. For illustrative purposes, the balance of this discussion is based only on the data for the fine-grained alloys. (More testing was conducted on them, and the data generally showed less scatter than for the coarse-grained alloys.)

The Larson-Miller parameter was calculated for each test conducted with the fine-grain-size alloys, using in turn the constants 19.8, 16.2, and 12.4. Because the calculations of the optimum constants were based on a curve-fitting method, the smallest range in parameter for any isostress condition would be expected when the constant and the parameters were determined for the same test data set (i.e., 19.8 for low $\overline{N}_V$, 16.2 for medium $\overline{N}_V$, and 12.4 for high $\overline{N}_V$). The variation of parameter range with the Larson-Miller constant used for an isostress condition is shown in table V. This table lists the maximum and minimum parameters calculated by using the three optimized constants. It also lists their temperature of occurrence and the range of parameters obtained at 30 000 psi (206 MN/m^2) for tests conducted between 1600° and 1800° F (871° and 982° C). For example, when the constant from the low-$\overline{N}_V$ alloy (19.8) is used in calculating parameters for the low-$\overline{N}_V$ alloy, the maximum parameter is 48.2×10^3 (at 1675° F (913° C)), and the minimum parameter is 47.6×10^3 (at 1800° F (982° C)), giving a parameter range of 0.6×10^3. When the same constant is used for the high-$\overline{N}_V$ alloy, the maximum parameter is 48.0×10^3 (at 1800° F (982° C)), and the minimum parameter is 46.1×10^3 (at 1600° F (871° C)). The range, therefore, is 1.9×10^3. It is evident from table V that the minimum range of parameters did occur when the constant was calculated for the data set in question. Further, it can be seen from the temperature of occurrence of the maximum and minimum parameters particularly for the high- and low-$\overline{N}_V$ data sets that the parameters become temperature-sensitive when the wrong constant is

TABLE V. - RANGE OF LARSON-MILLER PARAMETER FOR FINE-GRAINED IN-100

[Tests run at 30 000 psi (206 MN/m^2) and over temperature range of 1600° to 1800° F (871° to 982° C).]

Alloy type[d]	Constant								
	[a]19.8			[b]16.2			[c]12.4		
	Parameter	Temperature		Parameter	Temperature		Parameter	Temperature	
		°F	°C		°F	°C		°F	°C
Low $\overline{N}_v$:									
Maximum	48.2×10^3	1675	913	40.6×10^3	1600	871	32.8×10^3	1600	871
Minimum	47.6	1800	982	39.5	1800	982	30.9	1800	982
Parameter range, ΔP	.6	----	---	1.1	----	---	1.9	----	---
Medium $\overline{N}_v$:									
Maximum	48.3×10^3	1725	941	40.4×10^3	1675, 1725	913, 941	32.3×10^3	1675	913
Minimum	47.4	1600	871	39.9	1800	982	31.4	1800	982
Parameter range, ΔP	.9	----	---	.5	----	---	.9	----	---
High $\overline{N}_v$:									
Maximum	48.0×10^3	1800	982	39.8×10^3	1800	982	31.4×10^3	1725	941
Minimum	46.1	1600	871	38.7	1600	871	30.9	1600	871
Parameter range, ΔP	1.9	----	---	1.1	----	---	.5	----	---

[a]Optimized constant for low-$\overline{N}_v$ alloy.
[b]Optimized constant for medium-$\overline{N}_v$ alloy.
[c]Optimized constant for high-$\overline{N}_v$ alloy.
[d]$\overline{N}_v$ is average electron vacancy concentration.

used. For example, when a constant of 19.8 is used for the high-$\overline{N}_v$ alloy, the maximum parameter occurs at 1800° F (982° C), and the minimum occurs at 1600° F (871° C). The opposite occurs when 12.4 is used as the constant for the low-$\overline{N}_v$ alloy.

An understanding of the magnitude of the errors that may occur when predicting life of an unstable alloy by parametric methods can be gained by considering how the predicted life varies with the range of observed parameter. The Larson-Miller equation may be written as

$$\log t = \frac{P}{T + 460} - C \qquad (2)$$

Differentiating equation (2) at constant temperature gives

$$d(\log t) = \frac{dP}{T + 460} \tag{3}$$

which may also be stated as

$$\frac{dt}{t} = \frac{dP}{T + 460} \times 2.303 \tag{4}$$

From equation (4) it will be assumed that the relative variation in predicted life $\Delta t/t$ is directly proportional to the variation in parameter ΔP at a given temperature. If 1560° F (849° C) is used as the temperature for 10 000-hour life for the stable alloy at 30 000 psi (206 MN/m^2), equation (4) may be rewritten as

$$\frac{\Delta t}{t} \approx 1.14 \times 10^{-3} \Delta P \tag{5}$$

When 0.6 is used for ΔP (table V) in equation (5), the variation in predicted life of the stable (low $\overline{N}_v$) alloy at 1560° F (849° C) would be expected to be approximately 70 percent of the midrange life. The variation in predicted life for the most unstable alloy studied (high-$\overline{N}_v$ alloy) based on the constant calculated for the stable alloy (low-$\overline{N}_v$ alloy) is almost three times greater, being 220 percent of the midrange life.

Inspection of the stress-rupture data in table III in conjunction with figure 3 shows that one alloy type behaves essentially the same as another at temperatures where sigma will not form in an appreciable quantity prior to rupture. However, in the sigma-forming range, the sigma-forming alloys change behavior relative to sigma-free material. Therefore, if the test conditions used to establish the constants for the predicting parameter fail to include tests in the temperature range where sigma forms, or if tests are conducted only in that range, one could easily be misled when attempting to estimate long-time life from short-time data. Although the example shown previously (table V) used the Larson-Miller parameter, all the better known, time-temperature parameters can be analyzed in the same manner. These parameters would be expected to give analogous results because they also imply that rupture time is a single-valued function of temperature at constant stress. Since the more complex kinetics of the sigma phase formation is superimposed on the rupture kinetics, the time-temperature function would be expected to become more complex in an unstable alloy system.

SUMMARY OF RESULTS

The following results were obtained from a study of the effect of sigma formation on the stress-rupture life of the nickel-base superalloy IN-100.

1. Three levels of titanium and aluminum additions to a single master heat of IN-100 increased the concentrations from the low end of commercial specifications (approx. 5 percent Al, 4.2 percent Ti) to near the high end of the specifications (5.6 percent Al, 4.6 percent Ti). This caused the unstressed alloy to change from one that at the lowest concentrations of aluminum and titanium was sigma-free after 5000 hours at 1550° F (843° C), to one that at the highest concentration formed sigma in less than 24 hours at 1550° F (843° C).

2. Isothermal transformation studies of unstressed material showed that the alloy with the lowest aluminum and titanium contents investigated, when cast with either a coarse or fine grain size, formed no sigma in 2500 hours between 1300° and 1800° F (704° and 982° C). However, the alloy with the highest aluminum and titanium contents formed sigma at all temperatures examined between 1300° and 1800° F (704° and 982° C) when fine or coarse grained.

3. At 1525° F (829° C) and 30 000 psi (206 MN/m^2) the fine-grained alloy with the highest aluminum and titanium content had a rupture life of less than 10 percent of that expected by extrapolation of the 30 000-psi (206-MN/m^2) isostress line for the alloy with the lowest aluminum and titanium content to this same temperature. The two sigma-forming alloys studied had lower stress-rupture lives than the sigma-free alloy throughout the time-temperature realm where sigma forms. The strongly sigma-prone alloy had shorter stress-rupture lives than the moderately sigma-prone alloy where sigma forms. However, above the temperature range were sigma formed, the high aluminum and titanium alloys had slightly longer lives.

4. The average electron vacancy number $\overline{N}_v$ of the residual matrix, based on the PHACOMP concept for calculating the partition of elements in an alloy, when compared to reported critical average electron vacancy numbers, correctly predicted the formation of sigma in the IN-100 compositions investigated. Using a method similar to that of Woodyatt, Sims, and Beattie, the sigma-free material had an $\overline{N}_v$ of 2.27 to 2.32, the moderately sigma-prone alloy had an $\overline{N}_v$ of 2.47 to 2.51, and the strongly sigma-prone alloy had an $\overline{N}_v$ of 2.59 to 2.71. It should be noted, however, that the $\overline{N}_v$ variation was obtained by varying only Al and Ti.

5. Sigma-free, low-$\overline{N}_v$ IN-100, coarse-grained materials usually had longer stress-rupture lives in the temperature range (1300° to 1800° F, 704° to 982° C) than fine-grained materials. Sigma-prone, medium- and high-$\overline{N}_v$ IN-100, fine-grained materials usually had longer lives than coarse-grained materials in the 1300° to 1800° F (704° to 982° C) range.

6. Although increasing the aluminum and titanium concentration in the alloy decreased the rupture ductility, no effect of sigma phase on rupture ductility was established.

7. The prediction of stress-rupture life of an unstable form of an alloy using data from a stable form of the alloy, by commonly used methods of extrapolation, may dangerously overestimate the life of the unstable alloy and should therefore be avoided.

Lewis Research Center,
National Aeronautics and Space Administration,
Cleveland, Ohio, January 23, 1969,
129-03-01-03-22.

APPENDIX - CALCULATION OF AVERAGE ELECTRON VACANCY CONCENTRATION $\overline{N}_v$

The $\overline{N}_v$ numbers presented in this report have been computed by two techniques, the method of Boesch and Slaney (ref. 2), and the method of Woodyatt, Sims, and Beattie (ref. 9). Both methods have been updated since they were first reported. The method referred to in this paper as the Boesch and Slaney method assumes that the only compound formed is $(Ni_{0.95}Cr_{0.03}Mo_{0.02})_3$ (Al, Ti, Zr), instead of Ni_3 (Al, Ti) as reported in reference 2.

The values reported in the text for the method of Woodyatt, Sims, and Beattie and the description of the method were supplied in private communication with C. T. Sims and H. Murphy of General Electric Co., Schenectady, N. Y. Their contribution of this information is gratefully acknowledged. The use of this method is described as follows:

(1) Convert weight percent of melt chemistry to atomic percent.

(2) Assume boride forms of the chemistry $(Mo_{0.5}Ti_{0.15}Cr_{0.25}Ni_{0.1})_3B_2$. The molybdenum is therefore reduced by $3 \times 0.5 \times (B/2)$, the Ti by $3 \times 0.15 \times (B/2)$, the Cr by $3 \times 0.25 \times (B/2)$, and the Ni by $3 \times 0.1 \times (B/2)$. Set boron to zero.

(3) Assume that 50 percent of the carbon forms monocarbides in the following order: Ta, Cb, Ti, Zr. For IN-100 then, the Ti remaining after boride formation is reduced by C/2. This reduction will use the fraction of carbon available for MC formation in the alloys studied. Set carbon equal to 0.5 of original carbon.

(4) Assume that 50 percent of the carbon forms $M_{23}C_6$ carbide of the chemistry $Cr_{21}Mo_2C_6$. The chromium is further reduced by $21/6 \times C$ and the molybdenum by $2/6 \times C$. Set carbon equal to zero.

(5) Assume that gamma prime forms of the composition Ni_3(Al, Ti, 0.5 V, 0.03 Cr) where the vanadium and chromium are the original atomic percent of the alloy. The nickel, then, is reduced by $3 \times$ (Al + Ti + 0.5 V + 0.03 Cr). The vanadium is reduced by a factor of 0.5, and the chromium is reduced by a factor of 0.03. Set Al and Ti equal to zero.

(6) The residual Cr, Ni, Co, V, Mo, Fe, and Zr are scaled to 100 percent (called residual matrix).

(7) Compute $\overline{N}_v$ where

$$\overline{N}_v = \sum_{n=1}^{n=i} f_n N_{v,n}$$

and

f_n = fraction of n^{th} element in residual matrix

N_v of Ni = 0.61

N_v of Co = 1.71

N_v of Fe = 2.66

N_v of Mo, Cr = 4.66

N_v of V = 5.66

N_v of Zr = 6.66

REFERENCES

1. Lund, C. H.: Physical Metallurgy of Nickel-Base Superalloys. DMIC Rep. 153, Defense Metals Information Center, Battelle Memorial Inst., May 5, 1961, p. 19.
2. Boesch, William J.; and Slaney John S.: Preventing Sigma Phase Embrittlement in Nickel Base Superalloys. Metal Progress, vol. 86, no. 1, July 1964, pp. 109-111.
3. Wlodek, S. T.: The Structure of IN-100, Trans. ASM, vol. 57, no. 1, Mar. 1964, pp. 110-119.
4. Wile, George J.: Materials Considerations for Long Life Jet Engines. Paper 65-744, AIAA, Nov. 1965.
5. Ross, E. W.; René 100: A Sigma-Free Turbine Blade Alloy. J. Metals, vol. 19, no. 12, Dec. 1967, pp. 12-14.
6. Anon.: Alloys Castings, Investment, Corrosion and Heat Resistant, Nickel Base-10 Cr-15Co-3Mo-4.75Ti-5.5Al-0.95V, Vacuum Melted and Vacuum Cast. Aerospace Material Spec. No. 5397, Feb. 15, 1965.
7. Burke, J.: The Kinetics of Phase Transformations in Metals. Pergamon Press, 1965, p. 112 ff.
8. Mendelson, Alexander; Roberts, Ernest, Jr.; and Manson, S. S.: Optimization of Time-Temperature Parameters for Creep and Stress Rupture, with Application to Data from German Cooperative Long-Time Creep Program. NASA TN D-2975, 1965.
9. Woodyatt, L. R.; Sims, C. T.; and Beattie, H. J., Jr.: Prediction of Sigma-Type Phase Occurrence from Compositions in Austenitic Superalloys. Trans. AIME, vol. 236, No. 4, Apr. 1966, pp. 519-527.

NATIONAL AERONAUTICS AND SPACE ADMINISTRATION
WASHINGTON, D. C. 20546

OFFICIAL BUSINESS

FIRST CLASS MAIL

POSTAGE AND FEES PAID
NATIONAL AERONAUTICS AND
SPACE ADMINISTRATION

"The aeronautical and space activities of the United States shall be conducted so as to contribute . . . to the expansion of human knowledge of phenomena in the atmosphere and space. The Administration shall provide for the widest practicable and appropriate dissemination of information concerning its activities and the results thereof."

—NATIONAL AERONAUTICS AND SPACE ACT OF 1958

NASA SCIENTIFIC AND TECHNICAL PUBLICATIONS

TECHNICAL REPORTS: Scientific and technical information considered important, complete, and a lasting contribution to existing knowledge.

TECHNICAL NOTES: Information less broad in scope but nevertheless of importance as a contribution to existing knowledge.

TECHNICAL MEMORANDUMS: Information receiving limited distribution because of preliminary data, security classification, or other reasons.

CONTRACTOR REPORTS: Scientific and technical information generated under a NASA contract or grant and considered an important contribution to existing knowledge.

TECHNICAL TRANSLATIONS: Information published in a foreign language considered to merit NASA distribution in English.

SPECIAL PUBLICATIONS: Information derived from or of value to NASA activities. Publications include conference proceedings, monographs, data compilations, handbooks, sourcebooks, and special bibliographies.

TECHNOLOGY UTILIZATION PUBLICATIONS: Information on technology used by NASA that may be of particular interest in commercial and other non-aerospace applications. Publications include Tech Briefs, Technology Utilization Reports and Notes, and Technology Surveys.

Details on the availability of these publications may be obtained from:

SCIENTIFIC AND TECHNICAL INFORMATION DIVISION

NATIONAL AERONAUTICS AND SPACE ADMINISTRATION

Washington, D.C. 20546